Early Stage Kinetics in a Unified Model of Shear-Induced Demixing and Mechanical Shear Banding Instabilities

S. M. Fielding* and P. D. Olmsted

Polymer IRC and Department of Physics & Astronomy, University of Leeds, Leeds LS2 9JT, United Kingdom

(Received 15 July 2002; published 6 June 2003)

We present a unified model of shear-induced demixing and "mechanical" shear banding instabilities in polymeric and surfactant solutions, by combining a simple flow instability with a two-fluid approach to concentration fluctuations. Within this model, we calculate the "spinodal" limit of stability of initially homogeneous shear states to demixing/banding, and predict the selected length and time scales at which inhomogeneity first emerges after a shear start-up "quench" into the unstable region, finding qualitative agreement with experiment. Our analysis is the counterpart, for this driven phase transition, of the Cahn-Hilliard calculation for unsheared fluid-fluid demixing.

DOI: 10.1103/PhysRevLett.90.224501 PACS numbers: 47.20.Ft, 47.50.+d, 83.10.Gr

Complex fluids show a rich variety of flow-induced phase transitions and instabilities, the understanding of which is vital for control of morphology and stability during processing. Two intensely studied examples are (i) shear-enhanced concentration fluctuations or shear-induced demixing (SID) of marginally miscible polymer solutions [1,2], and (ii) shear banding (SB) in semidilute wormlike micellar surfactants (SDWMs) that have a constitutive curve (shear stress Σ_{xy} vs shear rate $\dot{\gamma}$) of the form ACEG in Fig. 1 [3]. In the regime of decreasing stress, CE, homogeneous flow is unstable [4] and the system splits into bands of differing shear rates $\dot{\gamma}_l$, $\dot{\gamma}_h$ [5,6], with a steady state flow curve ABFG.

While SB is often attributed purely this "*mechanical*" origin, in the negatively sloping constitutive curve [3,4], SID is usually seen as a flow-induced onset of the nearby *thermodynamic* demixing transition [1,2,7]. In this Letter, we conceptually *unify* these transitions by combining a simple flow instability (Fig. 1) with the "two-fluid model" [7–9] of flow-concentration coupling, as used previously to capture viscoelastic phase separation and SID in systems with monotonically increasing stress [10]. Within our unified model, we study the early stages of demixing/banding, by analogy with the Cahn-Hilliard (CH) analysis [11] for unsheared demixing, to find the "spinodal" onset of instability and the length (k^{*-1}) and time scale ($\tau_{\rm inst}$) at which inhomogeneity emerges after a shear start-up quench into the unstable regime.

Experimentally, shear start-up in SB SDWMs reveals a metastable regime $\dot{\gamma}_l < \dot{\gamma} \lesssim \dot{\gamma}_{c1}$ of slow band formation [12], and an unstable regime [13], $\dot{\gamma} \gtrsim \dot{\gamma}_{c1}$, where the stress can hugely overshoot its ultimate banded value, $\Sigma_{\rm sel}$, before subsiding rapidly to it. Notably, this overshoot often coincides with strongly enhanced *concentration fluctuations* [14] that emerge perpendicular to the shear compression axis, strongly resembling those seen at the same "anomalous" orientation in weakly sheared SID polymers [1] and (more recently) wormlike micelles [15]. These fluctuations can be quite strongly peaked [with $k^{*-1} \sim O(1\ \mu{\rm m})$ in Ref. [14]] suggesting that a CH-style analysis might be fruitful, as for SID in Ref. [7]. Further evidence for concentration coupling is the slight upward slope often seen in the *steady state* banding "plateau" BF [13,16], suggesting a concentration difference between the bands [17]. With this motivation, we combine a flow instability of the type shown in Fig. 1 with the two-fluid model for flow-concentration coupling.

The two-fluid model [8–10] considers separate force balance equations for the micelles (velocity $\underline{v}_m$) and solvent (velocity $\underline{v}_s$) in any solution element. The micelles are assumed to experience: (i) the viscoelastic backbone stress $\delta F/\delta \underline{\underline{W}} = G(\phi)\underline{\underline{W}}$ due to the local deviatoric micellar strain $\underline{\underline{W}}$, with modulus $G(\phi)$; (ii) the osmotic force $\phi \underline{\nabla} \delta F/\delta\phi$, where ϕ is the micellar volume fraction. This acts directly between "monomers," driving conventional micellar diffusion. The free energy

$$F = \frac{1}{2}\int d^3q(1+\xi^2q^2)f''|\phi(q)|^2 + \frac{1}{2}\int d^3x\, G(\phi)\,{\rm tr}\,\underline{\underline{\tilde{W}}}, \tag{1}$$

where f''^{-1} is the osmotic susceptibility, ξ the equilibrium correlation length for concentration fluctuations, and $\underline{\underline{\tilde{W}}} = \underline{\underline{W}} - \ln(\underline{\underline{\delta}} + \underline{\underline{W}})$. The micelles also feel (iii) Newtonian stress $2\phi\eta_m\underline{\underline{D}}^0_m$ from fast Rouse modes, with

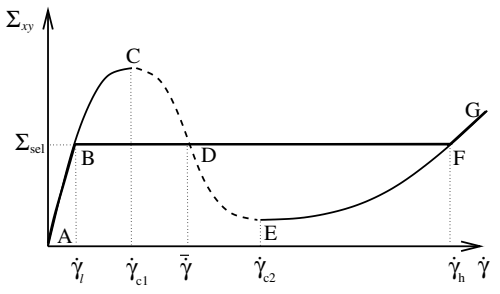

FIG. 1. Schematic constitutive curve showing flow instability.

viscosity η_m and (traceless) strain rate $\underline{\underline{D}}^0_m = \frac{1}{2}(\underline{\nabla}\,\underline{v}_m + \underline{\nabla}\,\underline{v}_m^T) - \frac{1}{3}\underline{\underline{\delta}}\,\underline{\nabla}\cdot\underline{v}_m$; and (iv) drag, $\zeta\underline{v}_{\rm rel}$, impeding motion relative to the solvent, $\underline{v}_{\rm rel} = \underline{v}_m - \underline{v}_s$. The solvent feels equal and opposite drag, and Newtonian stress $2(1-\phi)\eta_s\underline{\underline{D}}^0_s$.

Adding the micellar and solvent stresses, the overall force balance in the mean velocity $\underline{v} = \phi\underline{v}_m + (1-\phi)\underline{v}_s$ is

$$\rho(\partial_t + \underline{v}\cdot\underline{\nabla})\underline{v} \equiv \rho D_t\underline{v} = \underline{\nabla}\cdot G(\phi)\underline{\underline{W}} - \phi\underline{\nabla}\frac{\delta F(\phi)}{\delta\phi} + 2\underline{\nabla}\cdot\phi\,\eta_m\underline{\underline{D}}^0_m + 2\underline{\nabla}\cdot(1-\phi)\eta_s\underline{\underline{D}}^0_s - \underline{\nabla}p, \tag{2}$$

with the pressure p fixed by incompressibility. Subtraction of the micellar and solvent stresses gives an equation for the relative velocity $\underline{v}_{\rm rel}$, which in turn determines the concentration fluctuations [18]:

$$D_t\phi = -\underline{\nabla}\cdot\phi(1-\phi)\underline{v}_{\rm rel} = -\underline{\nabla}\cdot\frac{\phi^2(1-\phi)^2}{\zeta(\phi)}\left[\frac{\underline{\nabla}\cdot G(\phi)\underline{\underline{W}}}{\phi} - \underline{\nabla}\frac{\delta F}{\delta\phi} + \frac{2\underline{\nabla}\cdot\phi\,\eta\underline{\underline{D}}^0_m}{\phi} - \frac{2\underline{\nabla}\cdot(1-\phi)\eta_s\underline{\underline{D}}^0_s}{1-\phi}\right]. \tag{3}$$

The essence of the two-fluid model is that the viscoelastic stress $G(\phi)\underline{\underline{W}}$ appears *alongside* the familiar osmotic stress in this diffusion equation. This causes micelles to diffuse up gradients in $G(\phi)\underline{\underline{W}}$ and, hence, couples concentration to flow [9]. If the stress then increases with concentration ($dG/d\phi > 0$, assumed here), positive feedback occurs, causing net diffusion of micelles *up* their own concentration gradient. This mechanism causes shear-enhanced concentration fluctuations in systems close to demixing (SID) [7,8,10], and concentration coupling in SB systems (below and Refs. [19–21]). The overall rate of micellar diffusion is set by the kinetic drag coefficient $\zeta(\phi)$. The "raw" micellar diffusion coefficient (without flow-concentration coupling) is $\mathcal{D} \propto f''/\zeta(\phi)$.

The viscoelastic micellar strain $\underline{\underline{W}}$ is assumed to obey the nonlocal Johnson-Segalman (d-JS) model [22]:

$$\partial_t\underline{\underline{W}} = -(\underline{v}_m\cdot\underline{\nabla})\underline{\underline{W}} + a(\underline{\underline{D}}_m\cdot\underline{\underline{W}} + \underline{\underline{W}}\cdot\underline{\underline{D}}_m) + (\underline{\underline{W}}\cdot\underline{\underline{\Omega}}_m - \underline{\underline{\Omega}}_m\cdot\underline{\underline{W}}) + 2\underline{\underline{D}}_m - \frac{\underline{\underline{W}}}{\tau(\phi)} + \frac{l^2}{\tau(\phi)}\nabla^2\underline{\underline{W}}. \tag{4}$$

The terms in $\underline{v}_m$, $\underline{\underline{D}}_m$, and $\underline{\underline{\Omega}}_m$ describe convection, stretching, and rotation of the micelles by flow: $\underline{\underline{D}}_m$ and $\underline{\underline{\Omega}}_m$ are the symmetric and antisymmetric parts of the strain rate tensor $\underline{\nabla}\,\underline{v}_m$. The slip parameter a measures the fractional stretch of the micelles compared to the flow. For $|a| < 1$ (slip) the intrinsic constitutive curve can be nonmonotonic, as in Fig. 1, capturing a flow instability. The term $\underline{\underline{W}}/\tau$ describes relaxation of the micelles on the Maxwell time $\tau(\phi)$. The gradient term $\{l^2/[\tau(\phi)]\}\nabla^2\underline{\underline{W}}$ allows a steady banded stress to be calculated [23]. The length l could be set by the mesh size.

Using this "d-JS-ϕ" model, we study planar shear between plates at $y = \{0, L\}$ with $\underline{v} = v(y)\hat{\underline{x}}$. We assume boundary conditions $\partial_y\phi = \partial_y^3\phi = \partial_y\underline{\underline{W}} = 0$, no slip, and controlled strain rate, $\int_0^L dy\dot{\gamma}(y) = \text{const}$. We extract typical parameter values from rheological data at $\phi = 0.11$ for CTAB(0.3M)/$NaNO_3$/H_2O [14], and light scattering (DLS) data for CTAB/KBr/H_2O [24]. We calculate the drag $\zeta(\phi) = 6\pi\bar{\eta}\xi^{-2}$ [25], where $\bar{\eta} = \phi\eta_m + (1-\phi)\eta_s$. We extrapolate $G(\phi)$, $\tau(\phi)$, $\mathcal{D}(\phi)$, $\zeta(\phi)$, $\xi(\phi)$ to $\phi < 0.11$ using scaling laws for SDWMs, and set $G(0.11) = 1$, $\tau(0.11) = 1$, and $L = 1$. We fix a by comparing with Cates' microscopic model [3].

The stationary homogeneous constitutive curves $\Sigma_{xy} = G(\phi)W_{xy} + \bar{\eta}\,\dot{\gamma}$ (Fig. 2) have a region of negative slope ending in a "critical" point $\phi_c \approx 0.015$. CPCl/NaSal in brine [6] shows the same trend. To determine the stability of these homogeneous shear states to banding/demixing, we linearize in fluctuations $\sum_{\underline{k}}[\delta\dot{\gamma}, \delta\underline{\underline{W}}, \delta\phi]_{\underline{k}}e^{i\underline{k}\cdot\underline{r}+\omega_{\underline{k}}t}$ about them, considering for simplicity wave vectors $\underline{k} = k\hat{\underline{y}}$. The eigenvalues of the resulting stability matrix determine the dispersion relation of the growth rates. The lower (upper) spinodal lies where the largest branch ω_k of this relation first goes positive as the background homogeneous state is swept up (down) the intrinsic constitutive curve. The corresponding eigenvector $\underline{v}_k$ encodes the relative amplitudes $\delta\dot{\gamma}, \delta W_{ij}, \delta\phi$, determining whether separation occurs mainly in the mechanical variables $\dot{\gamma}, W_{ij}$ ("SB") or in concentration ("SID").

In the limit of infinite drag $\zeta \to \infty$ at fixed micellar diffusion coefficient $\mathcal{D} \propto f''/\zeta$, coupling of the mechanical variables $\delta\dot{\gamma}, \delta W_{ij}$ to fluctuations in concentration $\delta\phi$ is disabled. Homogeneous shear is then unstable to shear banding in the mechanical subspace $[\delta\dot{\gamma}, \delta W_{xy}, \delta W_{xx}, \delta W_{yy}]$ only if $d\Sigma_{xy}/d\dot{\gamma} < 0$: The spinodal is given by circles in Fig. 2. Independently, Eq. (3) (now reduced to the familiar CH equation) would have its own fluid-fluid demixing instability if $\mathcal{D} < 0$, but we consider only systems that are stable in zero shear, $\mathcal{D} > 0$.

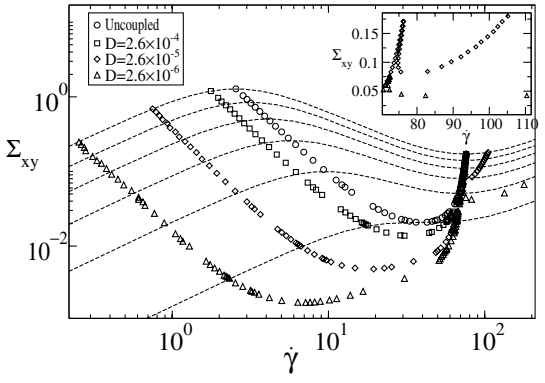

FIG. 2. Lines: Intrinsic constitutive curves for $\phi = 0.11$, 0.091, 0.072, 0.053, 0.034, and 0.015 (downwards). Symbols: Spinodals for the uncoupled limit $\zeta \to \infty$ at fixed $\mathcal{D} \propto f''/\zeta(\phi)$(○); coupled model with $\mathcal{D}(\phi = 0.11)$ from DLS (□), and artificially reduced $\mathcal{D}$ (◇, △).

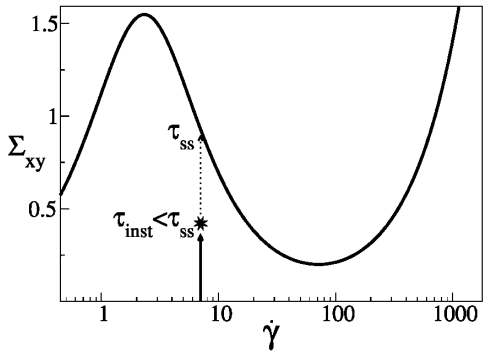

FIG. 3. Instability occurring as the homogeneous start-up flow evolves towards the intrinsic unstable constitutive curve.

For finite drag, flow-concentration feedback couples these subspaces and enhances the instability, which can now occur even if the uncoupled model is mechanically stable, $d\Sigma_{xy}/d\dot{\gamma} > 0$. For model parameters from the data of Refs. [14,24], this enhancement is only slight (squares in Fig. 2) so the instability is still essentially mechanical SB. Its eigenvector is still dominated by the mechanical variables $\delta\dot{\gamma}, \delta W_{ij}$ [19]. The enhancement increases strongly near a zero-shear demixing instability: The triangles in Fig. 2 are for a small, but still positive, (raw) diffusion coefficient $\mathcal{D}$. Here, instability sets in at very low shear rates, where it is now essentially SID [7,8,10], with an eigenvector dominated by $\delta\phi$ [26].

We now study the early-time kinetics after a shear start-up quench into the unstable regime. When the rheometer plate is set moving the shear rate rapidly homogenizes, on the Reynolds time scale $\rho L^2/\eta \ll \tau$. The shear stress $\Sigma_{xy}(t) = GW_{xy}(t) + \eta\dot{\gamma}$ then *starts* evolving towards the intrinsic constitutive curve, on the Maxwell time scale τ, with $\underline{\underline{W}}(t)$ *initially* given by the homogeneous start-up solution of Eq. (4). In the absence of instability, it would attain this constitutive curve at some time $\tau_{ss} = O(\tau)$. However, at some time $t_0 \leq \tau_{ss}$ a branch of the (now time-dependent) dispersion relation $\omega_k(t)$ goes unstable (positive). Indeed, τ_{ss} is, in general, longer than the growth time $1/\omega_k$ of the instability itself (except very near the spinodal), so the instability develops *before* the intrinsic constitutive curve can be attained (Fig. 3) [27]. The size of the growing fluctuations at $t > t_0$ is $A_k \sim \exp[\int_{t_0}^{t} dt'\, \omega_k(t')]$. A rough criterion for detectability is $\log A_k = O(10)$, which defines a k-dependent time $\tau_{\rm inst}(k)$ via $\int_{t_0}^{\tau_{\rm inst}(k)} dt'\, \omega_k(t') = O(10)$. In most regimes, fluctuations emerge fastest at a selected wave vector k^*, due to a peak in the dispersion relation $\omega_k(t)$ (below), so we define the overall time scale of the instability to be $\tau_{\rm inst} = \tau_{\rm inst}(k^*)$ (Fig. 3). For times $t > \tau_{\rm inst}$, the system is measurably inhomogeneous. Our linear calculation cannot predict subsequent behavior.

Figure 4 shows the time-dependent dispersion relation $\omega_k(t)$ for three unstable start-up flows. Figure 4(a) is for the pure mechanical (SB) instability ($\zeta \to \infty$ at fixed $\mathcal{D}$), i.e., inside the spinodal given by circles in Fig. 2. Here, the dispersion relation shows a broad plateau, with no clearly selected length scale. On the plateau, the growth rate ω_k is limited by that of viscoelastic stress response, $O(1/\tau)$, with a prefactor set by $-d\Sigma_{xy}/d\dot{\gamma}$. At higher $k \sim 1/l$, ω_k is cut off by interfaces; at low k (beyond typical gap sizes), $\omega_k \propto k^2$ due to inertial effects. A plateau is consistent with Ref. [28]. (The selected k^{*-1} found in Ref. [29] followed from an adiabatic viscoelastic stress, which artificially eliminated the plateau.) The temporal oscillation in Fig. 4(a) results from start-up oscillations in the homogeneous background $\underline{\underline{W}}(t)$. ($t \approx 2$ sees a minimum in $\underline{\underline{W}}$, though the instability actually develops before this; $\tau_{\rm inst} < 2$.)

For finite drag, concentration coupling enhances the instability at high k. (Small k modes are unaffected as concentration diffusion is slow over large distances.) In competition with the interfacial cutoff, this enhancement *selects a length scale* k^{*-1} [Figs. 4(b) and 4(c)], as seen experimentally [14].

Figure 4(b) is for a system far from zero-shear demixing (spinodal given by squares in Fig. 2), showing "SB, perturbed by concentration coupling": The eigenvector $\underline{v}_{k^*}$ is still mechanically dominated [19]. The wave vector

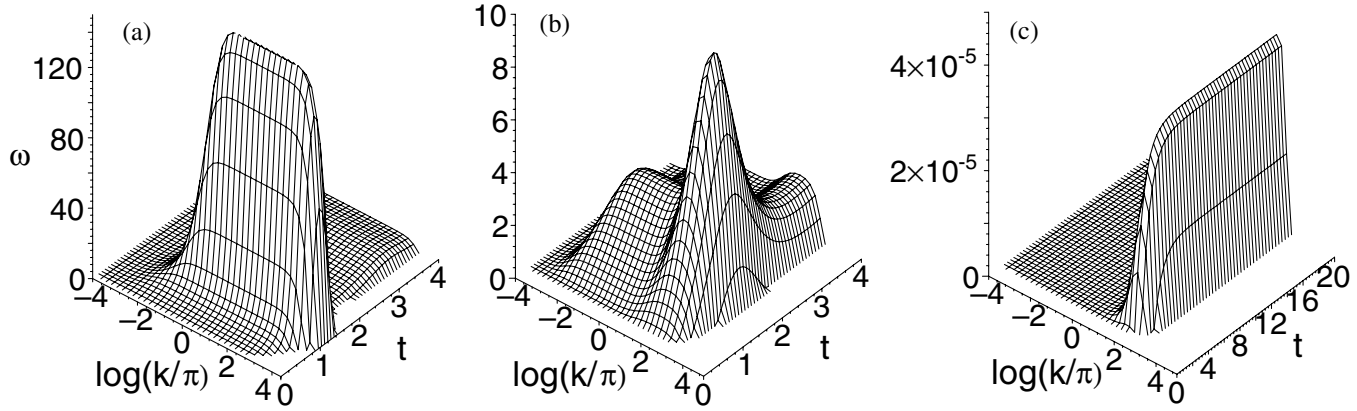

FIG. 4. Start-up dispersion relations, ω_k. (a) Uncoupled, $\dot{\gamma} = 7.0$, $\tau_{\rm inst} \approx 0.9$, no selected k^*. (b) $\mathcal{D} = 2.6 \times 10^{-4}$, $\dot{\gamma} = 4.0$, $\tau_{\rm inst} \approx 2.5$, $\log(k^*/\pi) \approx 1.8$. (c) $\mathcal{D} = 2.6 \times 10^{-9}$, $\dot{\gamma} = 0.01$, $\tau_{\rm inst} \gg 20$, $\log(k^*/\pi) \approx 1.5$.

k^* and time scale τ_{inst} are roughly comparable to those found by scattering in Ref. [14], from which the parameter values were taken.

Figure 4(c) is close to zero-shear demixing, $\mathcal{D} \gtrsim 0$, for which the lower spinodal (triangles in Fig. 2) is far below that of the pure mechanical instability. Our imposed shear rate is low (just inside this spinodal), so this instability is unaffected by the higher-shear regime, $d\Sigma_{xy}/d\dot{\gamma} < 0$. Indeed, the mechanical dispersion plateau that was still apparent in Fig. 4(b) (which was for stronger shear, with $d\Sigma_{xy}/d\dot{\gamma} < 0$) is now absent. Instead we see SID, dominated by $\delta\phi$, with $\omega = -\mathcal{D}_{\text{eff}}k^2$ for $k < k^*$. Although the *raw* diffusion coefficient $\mathcal{D} > 0$, $\mathcal{D}_{\text{eff}} < 0$ (unstable) due to the coupling between concentration and flow. At these low shear rates, the instability is slow enough that the intrinsic constitutive curve *is* reached before fluctuations grow appreciably. Higher-shear rates, where $d\Sigma_{xy}/d\dot{\gamma} < 0$, see a return to more violent concentration-coupled SB, dominated by $\delta\dot{\gamma}$, δW_{ij}.

Coupling of flow instabilities to concentration was first predicted by the remarkable insight of Ref. [17]. However, this directly assumed a chemical potential $\mu = \mu(\dot{\gamma})$. Although this is equivalent to our approach in the limit of adiabatic stress response, we have seen that instability does depend on the rate of viscoelastic stress response.

In summary, we have studied the early-time kinetics of shear banding in the d-JS model with two-fluid coupling to concentration. We find a smooth crossover from mechanical instability, signified by a negative constitutive slope $d\Sigma_{xy}/d\dot{\gamma} < 0$, to shear-induced demixing, according to the proximity to underlying zero-shear demixing. For start-up quenches deep in the unstable region the instability, in general, occurs before the homogeneous start-up flow can reach the intrinsic constitutive curve, unlike an equilibrium "quench," in which an unstable spinodal line can usually be attained [27]. No initial length scale is selected, *unless* the instability is coupled to concentration. These results are qualitatively consistent with experiments on wormlike micelles [14]; and suggest new experiments that can measure by, e.g., depolarized light scattering, the nature of the unstable eigenvector.

After this Letter was submitted, Yuan introduced a similar two-fluid shear banding model [21].

We thank R. Larson, S. Lerouge, and T. McLeish for discussions and EPSRC GR/N 11735 for funding.

*Electronic address: physf@irc.leeds.ac.uk

[1] X. L. Wu, D. J. Pine, and P. K. Dixon, Phys. Rev. Lett. **66**, 2408 (1991).
[2] H. Gerard, J. S. Higgins, and N. Clarke, Macromolecules **32**, 5411 (1999).
[3] M. E. Cates, J. Phys. Chem. **94**, 371 (1990); N. A. Spenley, M. E. Cates, and T. C. B. McLeish, Phys. Rev. Lett. **71**, 939 (1993).
[4] J. Yerushalmi, S. Katz, and R. Shinnar, Chem. Eng. Sci. **25**, 1891 (1970).
[5] H. Rehage and H. Hoffmann, Mol. Phys. **74**, 933 (1991); J. F. Berret, D. C. Roux, G. Porte, and P. Lindner, Europhys. Lett. **25**, 521 (1994); V. Schmitt, F. Lequeux, A. Pousse, and D. Roux, Langmuir **10**, 955 (1994); J. P. Decruppe, E. Cappelaere, and R. Cressely, J. Phys. II (France) **7**, 257 (1997); M. M. Britton and P. T. Callaghan, Phys. Rev. Lett. **78**, 4930 (1997).
[6] J. F. Berret, D. C. Roux, and G. Porte, J. Phys. II (France) **4**, 1261 (1994).
[7] S. T. Milner, Phys. Rev. E **48**, 3674 (1993).
[8] P.-G. de Gennes, Macromolecules **9**, 587 (1976); F. Brochard, J. Phys. (Paris) **44**, 39 (1983); M. Doi and A. Onuki, J. Phys. II (France) **2**, 1631 (1992); S. T. Milner, Phys. Rev. Lett. **66**, 1477 (1991); N. Clarke and T. C. B. McLeish, Phys. Rev. E **57**, R3731 (1998); N. Clarke, Faraday Discuss. **112**, 249 (1999).
[9] E. Helfand and G. H. Fredrickson, Phys. Rev. Lett. **62**, 2468 (1989).
[10] A. Onuki, R. Yamamoto, and T. Taniguchi, J. Phys. II (France) **7**, 295 (1997); J. L. Goveas and G. H. Fredrickson, J. Rheol. **43**, 1261 (1999); H. Tanaka, Phys. Rev. Lett. **76**, 787 (1996).
[11] A. J. Bray, in *Soft and Fragile Matter: Nonequilibrium Dynamics, Metastability and Flow*, edited by M. E. Cates and M. R. Evans (Institute of Physics, Bristol, 2000).
[12] C. Grand, J. Arrault, and M. E. Cates, J. Phys. II (France) **7**, 1071 (1997).
[13] J. F. Berret and G. Porte, Phys. Rev. E **60**, 4268 (1999).
[14] J. P. Decruppe, S. Lerouge, and J. F. Berret, Phys. Rev. E **6302**, 2501 (2001); S. Lerouge, J. P. Decruppe, and C. Humbert, Phys. Rev. Lett. **81**, 5457 (1998); S. Lerouge, Ph.D. thesis, University of Metz, 2000.
[15] I. A. Kadoma and J.W. van Egmond, Langmuir **13**, 4551 (1997); E. Wheeler, P. Izu, and G. G. Fuller, Rheol. Acta **35**, 139 (1996).
[16] J. F. Berret, D. C. Roux, and P. Lindner, Eur. Phys. J. B **5**, 67 (1998).
[17] V. Schmitt, C. M. Marques, and F. Lequeux, Phys. Rev. E **52**, 4009 (1995).
[18] We have omitted small inertial terms from Eq. (3) [19].
[19] S. M. Fielding and P. D. Olmsted, cond-mat/0208599.
[20] S. M. Fielding and P. D. Olmsted, cond-mat/0302098.Eur. Phys. J. E (to be published).
[21] X.-F. Yuan and L. Jupp, Europhys. Lett. **60**, 691 (2002).
[22] M. Johnson and D. Segalman, J. Non-Newtonian Fluid Mech. **2**, 255 (1977); P. D. Olmsted, O. Radulescu, and C.-Y. D. Lu, J. Rheol. **44**, 257 (2000).
[23] P. D. Olmsted and P. M. Goldbart, Phys. Rev. A **46**, 4966 (1992); J. R. A. Pearson, J. Rheol. **38**, 309 (1994).
[24] S. J. Candau, E. Hirsch, and R. Zana, J. Colloid Interface Sci. **105**, 521 (1985).
[25] P. G. de Gennes, *Scaling Concepts in Polymer Physics* (Cornell, Ithaca, 1975).
[26] The high shear lobe of instability is discussed in [19].
[27] For T quenches in demixing, the system essentially starts on the unstable branch of the chemical potential because rapid heat conduction occurs well before demixing.
[28] N. A. Spenley, X.-F. Yuan, and M. E. Cates, J. Phys. II (France) **6**, 551 (1996).
[29] J. K. G. Dhont, Phys. Rev. E **60**, 4534 (1999).